

# Super-Regenerative Receiver for OFDM Communication

F. Xavier Moncunill-Geniz, Jordi Bonet-Dalmau, Francisco del Águila-Lopez,  
Ilker Demirkol, Pere Palà-Schönwälder

Department of Mining, Industrial and ICT Engineering (EMIT), Manresa School of Engineering (EPSEM)  
Universitat Politècnica de Catalunya (UPC)  
08242 Manresa, Spain  
xavier.moncunill@upc.edu

**Abstract**—In this paper, we demonstrate the suitability of the super-regenerative receiver in OFDM communication. The well-known property of super-regenerative oscillators to preserve the amplitude and phase information is exploited to detect the OFDM symbols. A new super-regenerative architecture is presented that makes use of both an envelope detector and a phase detector connected at the output of the superregenerative oscillator. The peak-amplitude and phase samples of the generated RF pulses feed the digital processing blocks to extract the data. Through proof-of-concept simulations of a four-subcarrier QPSK OFDM modulation in the 2.4 GHz ISM band, we validate our proposed approach. This study paves the way to the use of low-power, low-cost super-regenerative receivers for widely-employed OFDM modulations.

**Index Terms**—OFDM communication, low-power RF receivers, super-regenerative receiver.

## I. INTRODUCTION

Orthogonal Frequency Division Multiplexing (OFDM) communication was introduced by Robert W. Chang of Bell Labs in 1966 [1]. Currently, it is being used in a wide range of communication technologies, both wired and wireless, such as ADSL broadband access, power-line communications, wireless local area communication, terrestrial digital TV and 4th and 5th generation mobile broadband standards. Among the advantages of this communication technique are: high spectral efficiency as compared to other modulation schemes, robustness against narrow-band co-channel interference and against intersymbol interference and fading caused by multipath propagation. It also supports efficient implementation using fast Fourier transform [2].

On the other hand, super-regenerative (SR) receivers (SRR) have proven to be very well-suited for wireless communications requiring low complexity, reduced cost, and low power consumption [3], [4]. Their simplistic design, which remained practically the same for decades, now benefits from the latest advances in electronic technology and in communication techniques. This is apparent from the recent studies on their CMOS integration, performance optimization via digital techniques, received-symbol synchronous operation, application to spread-spectrum (SS) and ultrawideband (UWB) communications [3]-

[6]. SRRs have traditionally been applied to the detection of amplitude-modulated signals. Recently, several proposals of SRRs adapted to detect phase and frequency have been developed [7] - [11]. The phase detection capability of SRRs opens a broad range of potential applications, such as the reception of OFDM-modulated signals, as targeted in this paper.

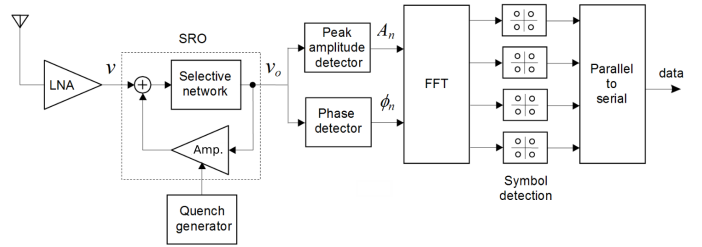


Fig. 1. Block diagram of the proposed SRR for OFDM-modulated signals.

## II. SUPER-REGENERATIVE RECEIVER ARCHITECTURE FOR OFDM COMMUNICATION

Fig. 1 shows the proposed SR architecture for the reception of OFDM-modulated signals. The receiver usually comprises of a low-noise amplifier (LNA) and a super-regenerative oscillator (SRO) that is implemented with a bandpass frequency selective network fed back through a variable gain amplifier. The gain of this amplifier is controlled by the quench signal producing alternated periods of system stability and instability. As a novelty over the previously proposed designs, this receiver includes both a peak-amplitude detector and a phase detector. The peak-amplitude detector can be implemented with a conventional envelope detector followed by a sample-and-hold circuit. The phase detector can be implemented in different ways. One of the simplest techniques reported performs SRO output pulse subsampling. The samples obtained are stored in the form of a vector in a shift register and subsequently processed, so that the comparison of the vector of samples in the current quench cycle with that of the previous cycle allow the detection of phase changes in a differential scheme [7], [8].

In the proposed architecture, a sample of the instantaneous amplitude and phase of the RF input signal is obtained in each

Work co-financed by the European Regional Development Fund of the European Union in the framework of the ERDF Operational Program of Catalonia 2014-2020 by the grant 001-P-001643 - Looming Factory.

quench cycle. The quench frequency must equal  $N$  times the OFDM symbol rate, where  $N$  is the number of subcarriers, so that  $N$  complex samples (amplitude and phase) of each symbol are obtained. The FFT of these samples is calculated to produce  $N$  complex samples in the frequency domain, which once decoded and serialized produce the original data bits. Note that the RF front end (LNA, SRO, peak amplitude and phase detectors in Fig. 1) that we propose can be used with any value of  $N$ , without affecting the power and area requirements of the front end.

### III. RECEPTION OF OFDM-MODULATED SIGNALS WITH SRR

#### A. Analytic description of OFDM modulation

In OFDM communications, the main stream of information bits is divided into  $N$  sub-streams, each one modulating a different subcarrier. Sub-stream bits are coded according to a specific QAM constellation as complex symbol coefficients

$$C_k = |C_k|e^{j\angle C_k}, \quad (1)$$

where the index  $k$  identifies the subcarrier number ( $0 \leq k \leq N-1$ ). The OFDM-modulated symbol in the time domain can be expressed as

$$v(t) = \sum_{k=0}^{N-1} |C_k| \cos(\omega_k t + \angle C_k), \quad (2)$$

expression that holds within a symbol period of duration  $T$  seconds, with  $\omega_k = 2\pi f_k$ , where

$$f_k = f_c + \left(k - \frac{N-1}{2}\right) \Delta f \quad (3)$$

represents the subcarrier frequency.  $f_c$  is the OFDM-modulation center frequency and  $\Delta f$  being the subcarrier spacing, i.e., the inverse of the OFDM symbol time  $T$ ,

$$\Delta f = \frac{\Delta\omega}{2\pi} = \frac{1}{T}. \quad (4)$$

At the receiver side,  $N$  samples of the OFDM symbol must be taken to decode the information associated to each subcarrier. Eventually, symbol shaping functions (e.g., raised cosine, Gaussian) may be used at the transmitter side to achieve specific spectral shapes and to concentrate energy around the sampling periods. In such a case, the expression of the modulated signal (2) can be written as

$$v(t) = \sum_{k=0}^{N-1} |C_k| \cos(\omega_k t + \angle C_k) \sum_{n=0}^{N-1} p_c(t - nT_s), \quad (5)$$

where  $T_s = T/N$  and the function  $p_c(t - n\frac{T}{N})$  describes the envelope of the  $n$ -th  $T_s$  interval of the OFDM symbol. The complex representation of the signal within this  $T_s$  interval is

$$\bar{V}_n(t) = p_c(t - nT_s) \sum_{k=0}^{N-1} C_k e^{j\omega_k t}. \quad (6)$$

#### B. Response of the SRO to an RF pulse

According to [12], the response in the linear mode of an SRO tuned to  $f_c$  to an input of the form

$$v(t) = p_c(t) \cos(\omega t + \phi) \quad (7)$$

is

$$v_o(t) = K |H(\omega)| p(t) \cos(\omega_c t + \phi + \angle H(\omega)), \quad (8)$$

where  $K$  is a peak amplification factor,  $H(\omega)$  is a normalized frequency response function,  $p(t)$  is the normalized envelope of the SRO output pulse and  $\omega_c = 2\pi f_c$  is the angular frequency of oscillation of the SRO. Equation (8) assumes that  $p_c(t)$  is zero beyond the limits of the quench period, of duration  $T_q$ , and that the instant of maximum sensitivity to the input signal is  $t = 0$ . This equation can be generalized to a quench cycle in which the maximum sensitivity is at the instant  $t = nT_q$ . Expressing the input as

$$v(t) = p_c(t - nT_q) \cos(\omega(t - nT_q) + \phi), \quad (9)$$

we get the response

$$v_o(t) = K p(t - nT_q) |H(\omega)| \times \cos(\omega_c(t - nT_q) + \phi + \angle H(\omega)), \quad (10)$$

The complex representation of (9)

$$\bar{V}(t) = p_c(t - nT_q) e^{j(\omega(t - nT_q) + \phi)} \quad (11)$$

produces the complex response

$$\bar{V}_o(t) = K p(t - nT_q) H(\omega) e^{j(\omega_c(t - nT_q) + \phi)}. \quad (12)$$

#### C. Response of the SRO to an OFDM-modulated signal

In the following, perfect synchronization will be assumed between the input pulse  $p_c(t - nT_s)$  and the  $n$ -th quench period, with  $T_q = T_s$ . According to (11) and (12), the response of an SRO with maximum sensitivity at  $t = nT_q$  to the OFDM-modulated signal (6) rewritten as

$$\bar{V}_n(t) = p_c(t - nT_q) \sum_{k=0}^{N-1} C_k e^{j((\omega_k(t - nT_q) + n\omega_k T_q))} \quad (13)$$

is

$$\begin{aligned} \bar{V}_{o,n}(t) &= K p(t - nT_q) \sum_{k=0}^{N-1} C_k H(\omega_k) e^{j(\omega_c(t - nT_q) + n\omega_k T_q)} \\ &= K p(t - nT_q) \left[ \sum_{k=0}^{N-1} C_k H(\omega_k) e^{jn\omega_k T_q} \right] e^{j(\omega_c(t - nT_q))}. \end{aligned} \quad (14)$$

#### D. Amplitude and phase detector outputs

The peak-amplitude detector samples the envelope of the SRO output pulses at the instant of maximum amplitude, i.e., when  $p(t - nT_q) = 1$ , yielding

$$A_n = K \left| \sum_{k=0}^{N-1} C_k H(\omega_k) e^{jn\omega_k T_q} \right|. \quad (15)$$

The phase detector provides the samples of the phase of the pulses relative to the sampling instant  $t = nT_q$  and to the SRO oscillation frequency  $\omega_c$ , i.e.,

$$\phi_n = \angle \left( \sum_{k=0}^{N-1} C_k H(\omega_k) e^{jn\omega_k T_q} \right). \quad (16)$$

Therefore, the complex samples associated to the detected amplitude and phase are

$$\bar{V}_{d,n} = A_n e^{j\phi_n} = K \sum_{k=0}^{N-1} C_k H(\omega_k) e^{jn\omega_k T_q}, \quad (17)$$

where considering (3)

$$\begin{aligned} \omega_k T_q &= \omega_c T_q - \left( \frac{N-1}{2} \right) \Delta\omega T_q + k\Delta\omega T_q \\ &= \omega_0 T_q + k\Delta\omega T_q. \end{aligned} \quad (18)$$

Taking into account that

$$\Delta\omega T_q = \frac{2\pi}{T} T_q = \frac{2\pi}{N}, \quad (19)$$

we can write

$$\begin{aligned} \bar{V}_{d,n} &= K e^{j\omega_0 T_q n} \sum_{k=0}^{N-1} C_k H(\omega_k) e^{j\frac{2\pi}{N} kn} \\ &= K e^{j\omega_0 T_q n} \times N \hat{c}_n, \end{aligned} \quad (20)$$

where the coefficient  $\hat{c}_n$  is the  $n$ -th sample in the time domain of the inverse discrete Fourier transform (IDFT) of  $C_k$  weighted by  $H(\omega_k)$ ,

$$\hat{c}_n = \text{IDFT} [C_k H(\omega_k)]. \quad (21)$$

The complex exponential preceding the summation in (20) can be eliminated by selecting an appropriate ratio between the frequency of the first subcarrier  $\omega_0$  and the quench frequency. Thus, by calculating a direct DFT, it is possible to obtain the estimated coefficients

$$\hat{C}_k = \text{DFT} [\hat{c}_n] = C_k H(\omega_k) = \text{DFT} \left[ \frac{\bar{V}_{d,n}}{KN} \right]. \quad (22)$$

The estimated coefficients  $\hat{C}_k$  will be a good approximation of the true coefficients  $C_k$  as long as  $H(\omega_k)$  is close to unity, as will happen in the vicinity of the maximum SRO amplification frequency  $\omega_c$ . Otherwise, deemphasis may be applied to the DFT calculation to correct the influence of  $H(\omega_k)$ .

#### IV. SIMULATION RESULTS

A simulation model was built on PathWave Advanced Design System (ADS) [13] based on the block diagram in Fig. 1. To exclusively evaluate the performance offered by the SR operation, idealized LNA, peak-amplitude and phase detectors were used. A testbench was built including OFDM signal generation, the OFDM SRR and a bit-error rate (BER) measurement modules. The set-up performs cosimulation of the digital blocks and the analog part of the SRR. The latter makes use of envelope simulation to reduce the simulation's time complexity.

Table I shows the OFDM-modulated signal parameters, whereas Table II lists the main SRR parameters chosen. The modulation center frequency is 2.45 GHz, with  $N = 4$  subcarriers and subcarrier spacing of 250 kHz, which corresponds to a symbol time  $T = 4 \mu\text{s}$ . Each subcarrier uses a QPSK modulation scheme. The SRO operates in the linear mode using a quench frequency of 1 MHz, so that 4 samples including both amplitude and phase of each OFDM symbol are obtained.

Fig. 2 shows the sensitivity function, the envelope of the pulses generated at the output of the SRO and the frequency selectivity curves obtained for the receiver with the parameters in Table II. Sawtooth and sinusoidal quench have been considered.

TABLE I  
OFDM SIGNAL ATTRIBUTES

Parameter	Value
Modulation center frequency	2.45 GHz
Symbol time	4 $\mu\text{s}$
Number of subcarriers	4
Subcarrier spacing	250 kHz
Subcarrier modulation scheme	QPSK
Data rate	2 Mbit/s

TABLE II  
SRR PARAMETERS

Parameter	Value
Reception center frequency	2.45 GHz
Quench waveform	sawtooth / sinusoidal
Quench frequency	1 MHz
OFDM symbol sampling rate	4 samples / symbol
LNA gain	20 dB
SRO quiescent quality factor	20
Mode of operation	linear
Total SRO peak gain	60 dB
-3-dB RF receiver bandwidth	
· sawtooth quench	4.07 MHz
· sinusoidal quench	4.47 MHz

Fig. 3 shows the instantaneous amplitude and phase of one OFDM symbol in the time domain generated with one different phase in each subcarrier from the four possible available values, according to a Gray encoding as follows:  $45^\circ$  ('00'),  $135^\circ$  ('01'),  $-135^\circ$  ('11') and  $-45^\circ$  ('10'). The oversampling ratio, i.e., the ratio between the number of samples used in the inverse DFT for the OFDM signal generation and the number of subcarriers, equals to 32. At  $t = nT_s$  ( $T_s = 1 \mu\text{s}$ ) the SRO samples the time domain values  $c_n$  of the frequency domain coefficients  $C_k$ .

Fig. 4 shows the samples provided by the peak-amplitude detector and the phase detector in the presence of noise, which quite accurately follow the values in Fig. 3 at the sampling instants. These samples, used in the FFT calculation and subsequent symbol decoding, exhibit a certain delay with respect to the sampling instants, in part due to the SRO signal build-up delay.

Finally, Fig. 5 plots the predicted BER curves with additive white Gaussian noise (AWGN) for the considered quench waveforms in two cases: with constant subcarrier amplitude, as defined by (2), and with an OFDM symbol shaped with a raised cosine  $p_c(t)$  (5) of period equal to the sampling period  $T_s$ . As can be seen, the latter achieves better results since it concentrates signal energy in the vicinity of the sensitivity periods of the SRO.

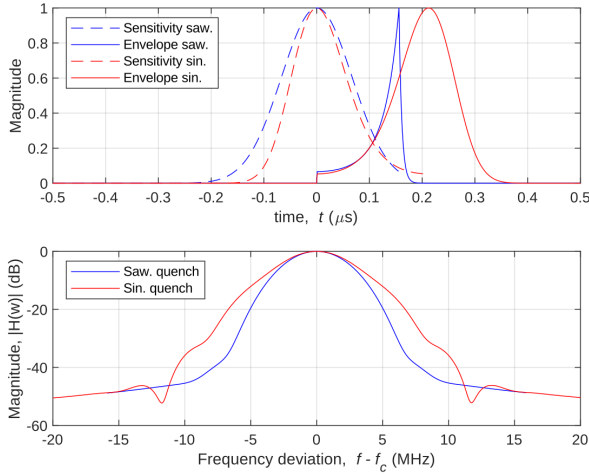


Fig. 2. Sensitivity function, SRO output pulse envelope (top) and frequency response (bottom) for sawtooth and sinusoidal quench.

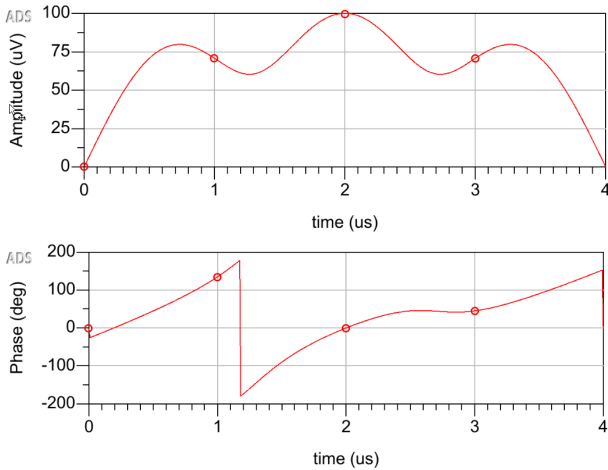


Fig. 3. Instantaneous amplitude and phase of the OFDM received symbol for the bit sequence '00011011' with an oversampling ratio of 32 and an average signal power of -73 dBm. The  $C_k$  coefficients are  $C_k = 100\sqrt{2} \mu V \times \{1\angle 45^\circ, 1\angle 135^\circ, 1\angle -45^\circ, 1\angle -135^\circ\}$ . The time domain values  $c_n$  are sampled at  $t = nT_s$  ( $T_s = 1 \mu s$ ). The values are  $c_n = 100\mu V \times \{0, \frac{1}{\sqrt{2}}\angle 135^\circ, 1, \frac{1}{\sqrt{2}}\angle 45^\circ\}$ .

## V. CONCLUSION

A novel architecture of SRR adapted to OFDM communication has been presented. It makes use of both a peak-amplitude detector and a phase detector to obtain several amplitude and phase samples of each OFDM symbol, which

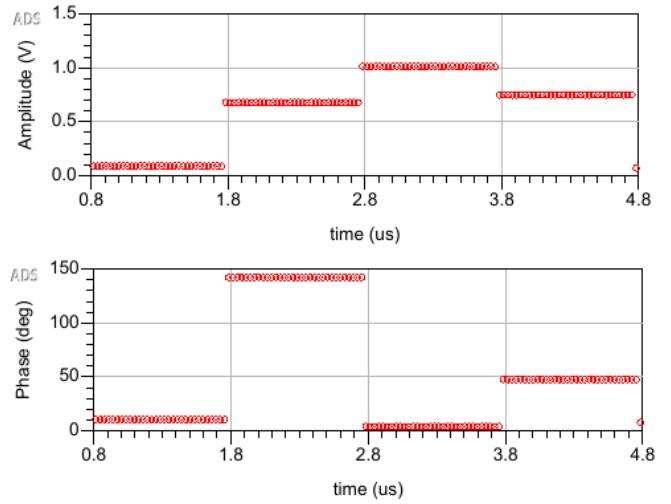


Fig. 4. Time domain values  $\hat{c}_n$  provided by the peak-amplitude detector and the phase detector when the SRR is sampling the OFDM signal in Fig. 3 in the presence of AWGN.

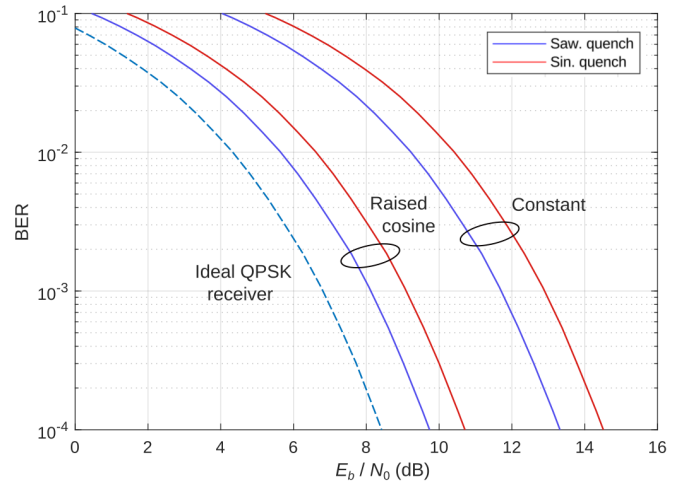


Fig. 5. Smooth BER curves for different OFDM symbol shaping functions: constant (Eq. (2)) and raised cosine (Eq. (5)). The ideal QPSK receiver curve would theoretically be achieved with a Gaussian shape matched to the sensitivity function of the SRO.

allows information bit decoding through FFT computation. Proof-of-concept simulation results on PathWave ADS with a four-subcarrier QPSK OFDM modulation in the 2.4 GHz ISM band validate the proposed approach. Hence, we claim that OFDM communications can benefit from the low-cost and low-power consumption features of SRR front ends, at the price of some sensitivity loss (1 to 6 dB in our simulation set-up) with respect to an ideal receiver.

## REFERENCES

- [1] S. B. Weinstein, "The history of orthogonal frequency-division multiplexing [History of Communications]," in *IEEE Communications Magazine*, vol. 47, no. 11, pp. 26-35, Nov. 2009, doi: 10.1109/MCOM.2009.5307460.

- [2] A. R. S. Bahai, B. R. Saltzberg, and M. Ergen, *Multi-Carrier Digital Communications. Theory and Applications of OFDM*, 2nd ed. Boston, U.S.A., Springer, 2004.
- [3] A. Vouilloz, M. Declercq, and C. Dehollain, "A low-power CMOS super-regenerative receiver at 1 GHz," *IEEE Journal of Solid-State Circuits*, vol. 36, no. 3, pp. 440-451, Mar. 2001.
- [4] J. Y. Chen, M. P. Flynn and J. P. Hayes, "A Fully Integrated Auto-Calibrated Super-Regenerative Receiver in 0.13- $\mu\text{m}$  CMOS," *IEEE Journal of Solid-State Circuits*, vol. 42, no. 9, pp. 1976-1985, Sept. 2007.
- [5] F. X. Moncunill-Geniz, P. Palà-Schönwälder, and F. del Águila-López, "New superregenerative architectures for direct-sequence spread-spectrum communications," *IEEE Trans. Circuits Syst. II, Exp. Briefs*, vol. 52, no. 7, pp. 415-419, Jul. 2005.
- [6] M. Pelissier, D. Morche and P. Vincent, "Super-Regenerative Architecture for UWB Pulse Detection: From Theory to RF Front-End Design," *IEEE Transactions on Circuits and Systems I: Regular Papers*, vol. 56, no. 7, pp. 1500-1512, July 2009.
- [7] P. Palà-Schönwälder, J. Bonet-Dalmau, F. X. Moncunill-Geniz, F. del Águila-López and R. Giralt-Mas, "A Superregenerative QPSK Receiver," in *IEEE Transactions on Circuits and Systems I: Regular Papers*, vol. 61, no. 1, pp. 258-265, Jan. 2014, doi: 10.1109/TCSI.2013.2268313.
- [8] P. Palà-Schönwälder, J. Bonet-Dalmau, A. López-Riera, F. X. Moncunill-Geniz, F. del Águila-López and R. Giralt-Mas, "Superregenerative Reception of Narrowband FSK Modulations," in *IEEE Transactions on Circuits and Systems I: Regular Papers*, vol. 62, no. 3, pp. 791-798, March 2015, doi: 10.1109/TCSI.2014.2382192.
- [9] D. Lee and P. P. Mercier, "A 1.65 mW PLL-free PSK receiver employing super-regenerative phase sampling," *2015 IEEE Biomedical Circuits and Systems Conference (BioCAS)*, 2015, pp. 1-4, doi: 10.1109/BioCAS.2015.7348307.
- [10] M. F. Wagdy, S. S. Rao, K. K. Singh and G. H. Ibrahim, "An 8-PSK receiver using an integrated low-noise amplifier & super-regenerative oscillator with digital detection technique," *2015 IEEE International Conference on Electronics, Circuits, and Systems (ICECS)*, 2015, pp. 416-420, doi: 10.1109/ICECS.2015.7440337.
- [11] H. Ghaleb et al., "A 180-GHz Super-Regenerative Oscillator with up to 58 dB Gain for Efficient Phase and Amplitude Recovery," in *IEEE Transactions on Microwave Theory and Techniques*, vol. 68, no. 6, pp. 2011-2019, June 2020, doi: 10.1109/TMTT.2020.2987555.
- [12] F. X. Moncunill-Geniz, P. Pala-Schonwalder and O. Mas-Casals, "A generic approach to the theory of superregenerative reception," in *IEEE Transactions on Circuits and Systems I: Regular Papers*, vol. 52, no. 1, pp. 54-70, Jan. 2005, doi: 10.1109/TCSI.2004.840095.
- [13] (2021, Nov.) PathWave Advanced Design System (ADS) website. [Online]. Available: <https://www.keysight.com/es/en/products/software/pathwave-design-software/pathwave-advanced-design-system.html>